2026 IEEE/SICE International Symposium on System Integration (SII)
January 11-14, 2026. Cancún, México

Local Velocity Field Control of a Nonholonomic Base for Kinesthetic Interaction with a Collaborative Arm

Tadej Petrič[1] and Leon Žlajpah[1]

Abstract— **This paper introduces a local control framework for mobile manipulators that enables coordinated motion between a nonholonomic base and a robotic arm without relying on any sensors mounted on the platform. The method is based on velocity vector fields defined in the mobile base frame and uses only internal joint measurements from the manipulator. A reduced kinematic model provides the translational end-effector (TEE) position, which drives all base motion decisions. By evaluating distance- and angle-based thresholds, the controller generates smooth linear and angular velocity commands that guide the base through extension, alignment, and retreat behaviors. The system supports real-time human interaction, such as kinesthetic guidance across the full reachable workspace, while respecting the nonholonomic constraints of the platform. Since the base controller is independent of the arm's control strategy, it is compatible with autonomous planning, teleoperation, or demonstration-based teaching. The proposed control strategy is particularly suited for collaborative scenarios where intuitive human guidance is essential and reliance on global localization is unnecessary. Experimental results with physical kinesthetic guidance demonstrate the platform's ability to reactively follow end-effector motion, preserving reachability and manipulability across the full workspace.**

I. INTRODUCTION

Mobile manipulators, which combine a robotic arm with a wheeled or tracked base, offer the potential to perform complex tasks in extended and partially structured environments. Their mobility allows access to spatially distributed workspaces, while their manipulators provide dexterous interaction with objects and tools. This makes them highly relevant for applications such as flexible manufacturing, logistics, inspection, assistive care, and collaborative robotics. However, achieving reliable and coherent behavior across the full joint workspace of the system remains a central challenge. The integration of nonholonomic constraints in the base, the redundancy introduced by combining two subsystems, and the coupling dynamics between them complicate motion coordination. These difficulties are even more pronounced in scenarios where global localization is unavailable, unreliable, or undesirable due to sensor occlusion, dynamic layouts, or the need for rapid reconfiguration.

Typical approaches for mobile manipulation rely on global planning techniques that attempt to find joint configurations by optimizing reachability, manipulability, or task efficiency. These include sampling-based, optimization-based, and search-based methods, which have been extensively research in recent literature [1]. While such approaches are effective in structured environments with accurate models and reliable localization, they often depend on precomputed motion plans or map-based infrastructure. As a result, they struggle to cope with real-time task variation or the unpredictability of human–robot interaction. In practice, many robotic applications demand immediate adaptation to disturbances, changes in the workspace, or contact events, for which global strategies are not responsive enough.

This limitation has shifted the focus toward reactive and local control strategies that use only internal sensing and onboard feedback to guide behavior. Several studies have emphasized the importance of adaptability and robustness over task efficiency, particularly in industrial and collaborative contexts [2], [3]. In such environments, robots must move smoothly, recover from disturbances, and maintain consistent performance despite uncertainties in perception and actuation. Reactive controllers that operate in the robot's local frame and rely solely on proprioceptive information have been shown to support safer, more natural behavior, especially in semi-structured settings such as construction sites or human-shared spaces [4], [5]. Moreover, recent works have highlighted the advantages of using reduced kinematic representations and local task-space control when dealing with physically interactive or sensor-limited systems [6], [7].

Various methods have attempted to bridge planning and control by incorporating base-arm coordination at different levels. For instance, task-space synchronization between the base and the manipulator can improve trajectory execution in constrained environments [8], while hierarchical controllers enable navigation through tight spaces by jointly considering obstacle proximity and kinematic feasibility [9]. Optimization-based schemes, such as capability-map planners [10] or hierarchical quadratic programming [11], allow prioritization of base and arm tasks in real time. Although these approaches improve integration between the subsystems, they often require accurate models, high computational resources, or tightly tuned control parameters. Similarly, model predictive controllers adapted to nonholonomic systems [12] and reactive dynamical systems methods [13] offer promising behavior but frequently rely on simplified assumptions that do not generalize well to real platforms.

Complementary insights from aerial robotics, where sensing is often limited and dynamics are uncertain, have shown that local control strategies can successfully manage complex behavior in manipulation scenarios. Surveys such as [14] demonstrate that even in high-uncertainty settings, reactive

*This research was funded by Slovenian Research Agency (ARIS) grant number P2-0076 and DIGITOP, GA no. TN-06-0106, funded by Ministry of Higher Education, Science and Innovation of Slovenia, Slovenian Research and Innovation Agency, and European Union – NextGenerationEU

[1]Tadej Petrič and Leon Žlajpah are with Jožef Stefan Institute, Department of Automatics, Biocybernetics and Robotics, Ljubljana, 1000, Slovenia {tadej.petric, leon.zlajpah}@ijs.si

control can maintain effective performance. On the ground, robust inverse kinematic formulations for hand-guidance under redundancy and singularity constraints have further illustrated how local task-space control enables intuitive behavior in physical interaction scenarios [15]. These insights reinforce the idea that robust and general control strategies should avoid dependencies on global pose estimation and instead rely on low-level geometric relationships and proprioception.

Despite this broad body of work, a persistent gap remains in the availability of unified and reactive control architectures that allow nonholonomic mobile manipulators to track full-workspace end-effector motion in real time without global localization or explicit planning. Many existing systems treat the mobile base and the arm as loosely coupled, resulting in disjointed or delayed responses, especially under fast manipulation, contact events, or kinesthetic teaching. This paper addresses that gap by introducing a control strategy based entirely on the relative pose between the base and the manipulator's TEE, computed from a reduced-order kinematic model that ignores wrist joints. The controller defines a velocity vector field in the base frame, using spatial thresholds to generate smooth, continuous linear and angular velocity commands that enable the platform to respond predictably to arm motion, even when guided by a human operator.

A key advantage of the proposed approach is that it requires no sensors or perception on the mobile base. The entire control loop depends solely on the manipulator's internal sensing, which is typically available from joint encoders. As such, the system can be used alongside autonomous planning, teleoperation, or kinesthetic demonstration. This decoupled design renders the method well suited for modular integration in dynamic scenarios or setups without platform-mounted sensing. It enables intuitive and compliant base motion by relying solely on the manipulator's internal state, while respecting the nonholonomic constraints of the mobile base. Experimental validation on a real robotic system demonstrates that the approach ensures stable and responsive behavior throughout diverse, physically guided trajectories, preserving consistent manipulability and smooth coordination across the full workspace.

II. CONTROL STRATEGY BASED ON LOCAL VELOCITY FIELDS

This section presents the proposed control approach, which governs the motion of a nonholonomic mobile base by relying exclusively on the relative position of the robot's TEE, expressed in the platform's local coordinate system. The main idea is to generate velocity commands using a spatially modulated vector field defined in the base frame. This method requires no sensors mounted on the mobile platform and depends solely on the internal joint measurements of the manipulator.

The full kinematic setup, reference frames, and control-relevant spatial regions are illustrated in Fig. 1. This figure provides a visual overview of the mobile manipulator system and serves as a reference for the spatial variables and zone-based activation scheme used throughout the control formulation.

The platform state is represented as $\mathbf{q}_b = [x_b, y_b, \theta]^\top$, capturing its position and orientation in the plane, while the arm configuration is denoted by $\mathbf{q}_m = [q_1, \ldots, q_n]^\top$, where n is the number of joints considered in a reduced-order model. This reduced model includes only the main positioning joints and omits distal joints, such as those in the wrist, which primarily affect orientation. The TEE position is obtained via forward kinematics and expressed in the mobile base frame $\mathcal{F}\mathrm{b}$, resulting in a locally defined control input $\boldsymbol{p} = [x, y, z]^\top$.

Four key geometric quantities are derived from $\boldsymbol{p}$: the distance to the end-effector, its angular deviation relative to the base heading, and two signed distance measures that trigger forward or backward motion. These quantities enable spatial modulation of the base's behavior, ensuring reactive and context-sensitive responses.

The signed distance to the outer boundary of the manipulator's workspace is defined as

$$d_\mathrm{f} = r_\mathrm{f} - \|\boldsymbol{p} - \mathbf{c}\|\,, \tag{1}$$

$$\mathbf{c} = \begin{bmatrix} 0 \\ 0 \\ l_0 \end{bmatrix}. \tag{2}$$

Here, $\mathbf{c}$ represents the center of a virtual spherical region, offset by l_0 in height, and $r_\mathrm{f} = l_1 + l_2$ denotes the maximum radial reach of the arm.

To prevent the manipulator getting too close to the platform, a second signed distance d_r is used to define a retreat region. This region is modeled as a vertical capsule surrounding the base

$$d_\mathrm{r} = b_d - \begin{cases} \|\boldsymbol{p}_\perp\| & \text{if } z \le l_0, \\ \|\boldsymbol{p} - \mathbf{c}\| & \text{if } z > l_0, \end{cases} \tag{3}$$

where $\boldsymbol{p}_\perp = [x, y]^\top$ projects the TEE position onto the ground plane. These two measures, d_f and d_r, determine whether the platform should remain stationary, move forward to extend reach, or retreat to preserve safety.

The linear velocity command v is defined as

$$v = \begin{cases} -K_r \cdot (\Delta_\mathrm{r} - d_\mathrm{r}) & \text{if } d_\mathrm{r} < \Delta_\mathrm{r}, \\ K_f \cdot (\Delta_\mathrm{f} - d_\mathrm{f}) & \text{if } d_\mathrm{f} < \Delta_\mathrm{f} \text{ and } d_\mathrm{r} \ge \Delta_\mathrm{r}, \\ 0 & \text{otherwise}, \end{cases} \tag{4}$$

where Δ_f and Δ_r denote threshold values for the forward and retreat zones, respectively, and K_r, K_f are proportional gains. This formulation ensures that the base reacts proportionally to how far the TEE has entered either zone.

The orientation of the platform is adjusted using the planar angle $\varphi = \arctan 2(y, x)$, which represents the direction of the TEE with respect to the base. To maintain smooth heading adjustments, a nonlinear activation function is applied to generate the angular velocity

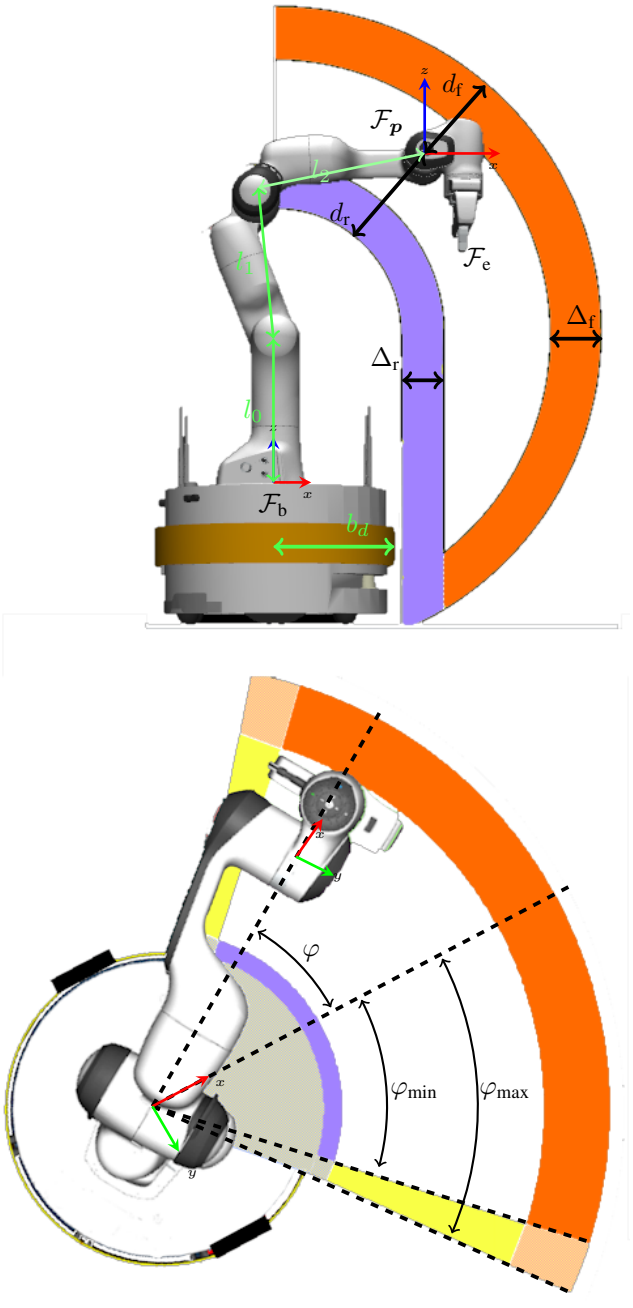

Fig. 1: The **top image** shows the robot's kinematic structure together with the spatial control zones. It includes the Franka Emika arm on a Tiago mobile base, with frames $\mathcal{F}\mathrm{b}$, $\mathcal{F}\boldsymbol{p}$, and $\mathcal{F}\mathrm{e}$, and control-relevant parameters l_0, l_1, l_2, and b_d. The retreat and forward zones are defined via signed distances d_r and d_f. The **bottom image** presents a top-down view for computing the angular deviation φ, with thresholds φ_min and φ_max defining the rotation activation region. Color-coded areas indicate control modes: purple (retreat), orange (extension), yellow (rotation), and their combinations.

$$\omega = K_\omega \cdot \mathrm{sign}(\varphi) \cdot \gamma(|\varphi|), \tag{5}$$

where K_ω is the angular control gain, and $\gamma(|\varphi|)$ is defined as

$$\gamma(|\varphi|) = \begin{cases} 0 & \text{if } |\varphi| \le \varphi_\mathrm{min}, \\ 3s^2 - 2s^3 & \text{if } \varphi_\mathrm{min} < |\varphi| < \varphi_\mathrm{max}, \\ 1 & \text{if } |\varphi| \ge \varphi_\mathrm{max}, \end{cases} \tag{6}$$

$$s = \frac{|\varphi| - \varphi_\mathrm{min}}{\varphi_\mathrm{max} - \varphi_\mathrm{min}}.$$

To reduce noise and ensure signal continuity, both velocity signals are passed through an exponential smoothing filter

$$\hat{v}_k = (1-\alpha)v_{k-1} + \alpha v_k, \tag{7}$$
$$\hat{\omega}_k = (1-\alpha)\omega_{k-1} + \alpha\omega_k, \tag{8}$$

followed by a rate limiter that enforces acceleration and velocity bounds

$$\tilde{v}_k = \psi_{v_\mathrm{max}}\left(v_{k-1} + \psi_{\Delta v_\mathrm{max}}(\hat{v}_k - v_{k-1})\right), \tag{9}$$
$$\tilde{\omega}_k = \psi_{\omega_\mathrm{max}}\left(\omega_{k-1} + \psi_{\Delta\omega_\mathrm{max}}(\hat{\omega}_k - \omega_{k-1})\right), \tag{10}$$

using the saturation function

$$\psi_r(x) = \begin{cases} -r & \text{if } x < -r, \\ x & \text{if } -r \le x \le r, \\ r & \text{if } x > r. \end{cases} \tag{11}$$

The final command sent to the platform is given by

$$\mathbf{u}_b = \begin{bmatrix} \tilde{v}_k \\ \tilde{\omega}_k \end{bmatrix}. \tag{12}$$

By relying exclusively on internal manipulator sensing and expressing all quantities in the base frame, the proposed controller ensures reactive and smooth motion without the need for global information or external sensors. The mobile platform remains passive while the manipulator operates within its effective workspace and activates only when necessary, supporting robust operation even under kinesthetic guidance or physical interaction.

III. SPATIAL ANALYSIS OF THE LOCAL VELOCITY FIELD

To gain further insight into the behavior of the proposed velocity control framework, we perform a spatial evaluation of the vector field across the robot's reachable volume. This analysis reveals how the control logic responds to different positions of the TEE, particularly with respect to the workspace boundaries and the immediate vicinity of the base. The vector field is evaluated over a discretized three-dimensional grid, where each point corresponds to a hypothetical position of the TEE, expressed as $\boldsymbol{p} = [x, y, z]^\top$ in the base coordinate frame. For each point, the linear

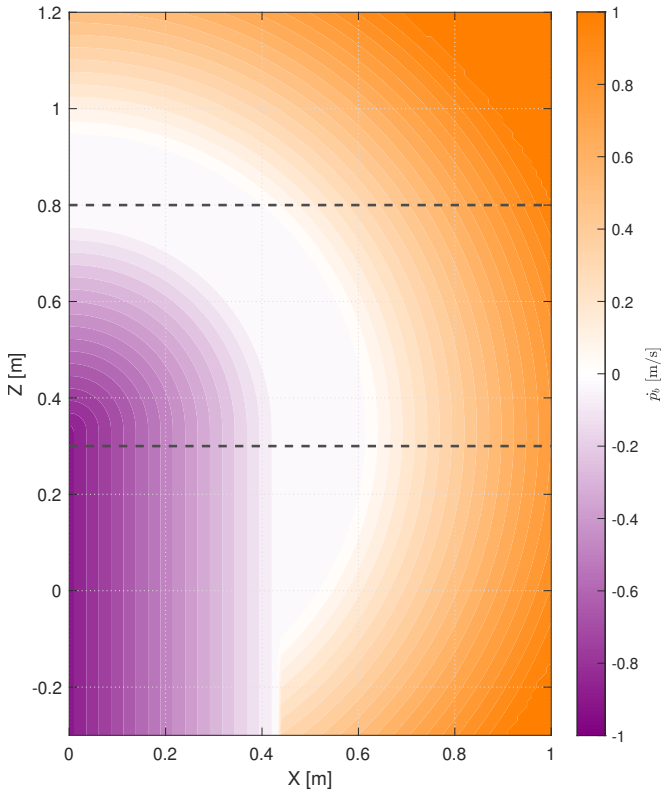

Fig. 2: Side view of the velocity field in the X–Z plane at $y = 0$. The color encodes the linear velocity command v as a function of the TEE position $\boldsymbol{p}$. Purple regions indicate backward motion (retreat), orange regions indicate forward motion (extension), and white regions represent passive states near the base. Dashed horizontal lines mark the specific z-levels at which top-down slices are shown in Fig. 3, providing spatial context for interpreting the layered structure of the field.

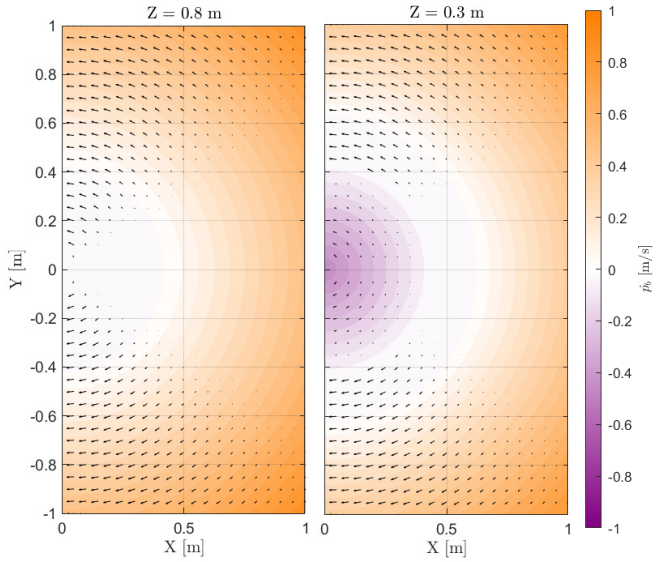

Fig. 3: Top-down views of the velocity field in the X–Y plane at two different heights: $z = 0.8$ and $z = 0.3$. The color map indicates the commanded linear velocity v, while arrows show the direction and strength of the angular velocity component ω. These plots illustrate how the platform transitions between retreat, passive, and extension behaviors depending on the horizontal position of the end-effector at different vertical levels.

velocity command v is computed directly using the spatial activation scheme defined by the signed distances d_{f} and d_{r}, as introduced in Section II. These quantities determine whether the platform should remain passive, move forward to extend its reach, or retreat to maintain a safe posture near its body.

Fig. 2 presents a side view (X–Z plane) of the spatially defined linear velocity field, corresponding to a fixed slice at $y = 0$. The color encodes the commanded linear velocity v: orange regions correspond to forward motion (positive v), purple regions indicate backward motion (negative v), and white regions represent passive zones near the center of the reachable space. This visualization reveals the vertical structure of the motion policy and illustrates how extension and retreat regions are distributed with respect to height. To further interpret the controller's response in horizontal layers of the workspace, we examine top-down views of the velocity field in the X–Y plane at two representative heights. Fig. 3 shows the velocity map at $z = 0.8$ and $z = 0.3$. In each slice, the background color represents the linear velocity v, while superimposed arrows depict the direction and relative magnitude of the angular velocity ω generated by the heading control policy.

This layered visualization clearly shows the separation between retreat, passive, and extension zones, governed by the thresholds Δ_{r} and Δ_{f}. The central region around the base exhibits zero velocity, corresponding to the passive zone where the manipulator operates comfortably within reach. As the TEE approaches the retreat region, negative velocities are activated, pushing the base away from potential collision. Similarly, as the end-effector nears the edge of the reachable workspace, positive velocities emerge, pulling the platform forward to maintain reachability. Importantly, the orientation vectors transition smoothly across the entire domain. Around the angular alignment thresholds $\varphi_{\min}$ and $\varphi_{\max}$, we observe a gradual buildup of rotational commands, confirming that the nonlinear angular control law provides a continuous and stable heading response. No abrupt changes or discontinuities are observed in the field, demonstrating the effectiveness of the cubic interpolation and smoothing mechanisms introduced in the controller.

Together, these visual analyses provide a spatially grounded validation of the proposed control strategy. The results confirm that the system exhibits predictable and robust transitions between motion states across a wide range of end-effector positions. The use of signed distances and smooth activation functions enables context-aware behavior and avoids abrupt switches, making the approach well suited for real-time operation in dynamic, unstructured environments.

Fig. 4: Sequence of kinesthetic guidance. As the operator physically moves the robot arm, the mobile base responds automatically by following the end-effector to maintain manipulability. This sequence corresponds to the experimental demonstration shown in Supplementary Multimedia 1.

A. Kinesthetic Teaching and Reactive Base Control through Local End-Effector Feedback

This experiment demonstrates how the proposed control strategy enables intuitive human–robot interaction by leveraging kinesthetic teaching. In this mode, the user physically guides the robot arm through free-space motion while the mobile base autonomously adapts its position in real time. The Franka Emika manipulator operates in a gravity-compensated mode, allowing the user to move the end-effector with minimal effort. Throughout the interaction, the control system evaluates the position of the TEE in the mobile base frame and generates velocity commands based on the local spatial context.

The robot's behavior in this scenario illustrates the essence of the proposed framework: continuous adaptation to the end-effector position without requiring any direct control inputs for the platform. When the TEE approaches the outer workspace boundary, the mobile base advances to preserve reachability. When the manipulator is pulled too close to the base, the platform retreats to avoid unfavorable configurations near its own body. If the TEE deviates significantly from the forward axis, the base also rotates to realign itself smoothly.

A key aspect of this demonstration is that all base motion is driven purely by proprioceptive sensing. The system requires no external tracking, global localization, or environmental models, which makes it especially suitable for unstructured or dynamic environments, as well as for intuitive physical teaching without additional infrastructure. Notably, the manipulator and base controllers function independently: the arm can be freely guided by the user, while the base reacts automatically based on the TEE position expressed in the local frame. This decoupled structure simplifies system integration and enables flexible use across different interaction paradigms. Fig. 4 presents a representative sequence from the experiment. As the user moves the end-effector across the workspace, the mobile base follows accordingly, maintaining appropriate spacing and alignment. The result is a fluid whole-body response that facilitates teaching by demonstration and lays the foundation for shared autonomy or collaborative task learning.

IV. DISCUSSION AND CONCLUSION

The control strategy presented in this paper offers a fully local and reactive solution for coordinating a nonholonomic mobile base with a manipulator, addressing common limitations of global planning methods and model-dependent control schemes. Unlike trajectory planning approaches that rely on precomputed paths or full-environment maps, our method generates velocity commands in real time using only internal feedback from the manipulator. This makes it inherently responsive and robust to unexpected disturbances or changes in the environment.

In contrast to dynamic systems-based or predictive control strategies, which often neglect the nonholonomic nature of wheeled platforms or require accurate system models, our formulation explicitly embeds kinematic constraints into a spatially modulated velocity field. This ensures that the resulting motion commands remain feasible and smooth across the entire workspace, including regions near the base or close to workspace boundaries.

By leveraging a reduced-order kinematic model and simple geometric primitives, the proposed approach achieves computational efficiency without sacrificing task relevance. It avoids the overhead of optimization-based or predictive frameworks while still enabling behavior such as reach extension, collision-aware retreat, and smooth heading alignment. Moreover, the control policy remains agnostic to how the manipulator is driven, allowing seamless integration with teleoperation, autonomous planning, or kinesthetic teaching.

This local and modular design makes the system especially well-suited for human-centered environments, where adaptability and safety are essential. It provides an intuitive mechanism for whole-body motion coordination without requiring additional sensors on the base or reliance on external localization systems.

In future work, this approach could be extended to multi-robot collaboration or integrated with local perception modules to enable more advanced interaction strategies. Its lightweight computational footprint and purely proprioceptive nature also suggest suitability for deployment on compact, mobile robotic systems operating in dynamic and partially known environments.

REFERENCES

[1] T. Sandakalum and M. H. Ang, "Motion Planning for Mobile Manipulators—A Systematic Review," *Machines*, vol. 10, no. 2, 2022.

[2] R. Bostelman, T. Hong, and J. Marvel, "Survey of research for performance measurement of mobile manipulators," *Journal of Research of the National Institute of Standards and Technology*, vol. 121, pp. 342–366, 2016.

[3] N. Ghodsian, K. Benfriha, A. Olabi, V. Gopinath, and A. Arnou, "Mobile Manipulators in Industry 4.0: A Review of Developments for Industrial Applications," *Sensors*, vol. 23, no. 19, 2023.

[4] P. Štibinger, G. Broughton, F. Majer, Z. Rozsypálek, A. Wang, K. Jindal, A. Zhou, D. Thakur, G. Loianno, T. Krajník, and M. Saska, "Mobile manipulator for autonomous localization, grasping and precise placement of construction material in a semi-structured environment," *IEEE Robotics and Automation Letters*, vol. 6, no. 2, pp. 2595–2602, 2021.

[5] Y. Qin, A. Escande, F. Kanehiro, and E. Yoshida, "Dual-arm mobile manipulation planning of a long deformable object in industrial installation," *IEEE Robotics and Automation Letters*, vol. 8, no. 5, pp. 3039–3046, 2023.

[6] Z. Zhou, X. Yang, H. Wang, and X. Zhang, "Coupled dynamic modeling and experimental validation of a collaborative industrial mobile manipulator with human-robot interaction," *Mechanism and Machine Theory*, vol. 176, p. 105025, 2022. [Online]. Available: https://www.sciencedirect.com/science/article/pii/S0094114X22002737

[7] J. Liu, Y. Deng, Y. Liu, L. Chen, Z. Hu, P. Wei, and Z. Li, "A logistic-tent chaotic mapping levenberg marquardt algorithm for improving positioning accuracy of grinding robot," *Scientific Reports*, vol. 14, no. 1, p. 9649, 2024. [Online]. Available: https://doi.org/10.1038/s41598-024-60402-1

[8] S. Zhou, Y. C. Pradeep, M. Zhu, K. Amezquita-Semprun, and P. Chen, "Motion Control of a Nonholonomic Mobile Manipulator in Task Space," *Asian Journal of Control*, vol. 20, no. 5, pp. 1745–1754, 2018.

[9] M. Mashali, L. Wu, R. Alqasemi, and R. Dubey, "Controlling a Non-Holonomic Mobile Manipulator in a Constrained Floor Space," *Proceedings - IEEE International Conference on Robotics and Automation*, pp. 725–731, 2018.

[10] H. Zhang, Q. Sheng, Y. Sun, X. Sheng, Z. Xiong, and X. Zhu, "A novel coordinated motion planner based on capability map for autonomous mobile manipulator," *Robotics and Autonomous Systems*, vol. 129, p. 103554, 2020. [Online]. Available: https://doi.org/10.1016/j.robot.2020.103554

[11] S. Kim, K. Jang, S. Park, Y. Lee, S. Y. Lee, and J. Park, "Whole-body control of non-holonomic mobile manipulator based on hierarchical quadratic programming and continuous task transition," *2019 4th IEEE International Conference on Advanced Robotics and Mechatronics, ICARM 2019*, no. April, pp. 414–419, 2019.

[12] K. Belda and O. Rovny, "Predictive control of 5 DOF robot arm of autonomous mobile robotic system motion control employing mathematical model of the robot arm dynamics," *Proceedings of the 2017 21st International Conference on Process Control, PC 2017*, pp. 339–344, 2017.

[13] L. P. Ellekilde and H. I. Christensen, "Control of mobile manipulator using the dynamical systems approach," *Proceedings - IEEE International Conference on Robotics and Automation*, pp. 1370–1376, 2009.

[14] X. Meng, X. Meng, Y. He, J. Han, and J. Han, "Survey on Aerial Manipulator: System, Modeling, and Control," *Robotica*, vol. 38, no. 7, pp. 1288–1317, 2020.

[15] M. Weyrer, M. Brandstötter, and M. Husty, "Singularity avoidance control of a non-holonomic mobile manipulator for intuitive hand guidance," *Robotics*, vol. 8, no. 1, pp. 1–17, 2019.